 https://doi.org/10.3311/PPch.20797

Periodica Polytechnica Chemical Engineering, 67(1), pp. 104–115, 2023

Modeling the Biosurfactant Fermentation by *Geobacillus stearothermophilus* DSM2313

Réka Czinkóczky[1], Áron Németh[1*]

[1] Department of Applied Biotechnology and Food Science, Faculty of Chemical Technology and Biotechnology, Budapest University of Technology and Economics, Műegyetem rkp. 3., H-1111 Budapest, Hungary
[*] Corresponding author, e-mail: naron@f-labor.mkt.bme.hu

Received: 08 July 2022, Accepted: 23 September 2022, Published online: 09 January 2023

Abstract

Biosurfactants are emerging molecules in the 21st century. However, their production intensification is still required for the development of feasible bioprocesses. Therefore, this paper studies a new biosurfactant-producer, namely *Geobacillus stearothermophilus* DSM2313 during statistical optimization via response surface methodology. After the statistical analysis the optimal pH = 7, glucose = 50 g/L and NH_4NO_3 = 2 g/L concentrations were determined. The biosurfactant production of the bacteria was predicted by our developed artificial neural network. The optimal harvesting time of the broth and the emulsification index values can be predicted simultaneously with the constructed artificial neural network. The best experiment was also kinetically described, and kinetic constants observed. Surface tension and emulsification activity were measured to characterize the formed products' efficiency. Based on these results, biosurfactants from *Geobacillus stearothermophilus* DSM2313 can act as bioemulsifier and can be applied for example in microbial enhanced oil recovery.

Keywords

biosurfactant, bioemulsifier, response surface methodology, kinetic modeling, artificial neural network

1 Introduction

Biosurfactants are amphiphilic molecules consisting of hydrophobic and hydrophilic groups, which were produced by different microorganisms (bacteria, yeasts and filamentous fungi), and can act on the interfaces between fluid phases with different degrees of polarity (oil/water) [1]. The widespread application of biosurfactants proved that they can substitute chemically synthesized surfactants. They can be applied in agriculture as pesticides [2, 3], in laundry detergents [4], in cosmetics formulations [5], in the food industry as emulsifiers [6], in the pharmaceutical industry as delivery systems [7, 8]. Due to their amphiphilic properties, biosurfactants facilitate the remediation of petroleum from the ecosystem. They decrease the interfacial tension and disperse the oil particles into small droplets, turning them into non-toxic materials [9]. The oil recovery from the petroleum wells (microbial enhanced oil recovery (MEOR)) has been enhanced by biosurfactants and their transport through sand pack columns and metal pipes which technic has been applied in the field [10]. The application of biosurfactants has many advantages over chemically produced surfactants, such as high biodegradability and low ecotoxicity, as well as can be easily produced from renewable raw materials [3]. Most chemical surfactants are derived from the petrochemical industry with a low production cost and high yield. However, this form of production is widely seen as unsustainable in the 21st century's circular ecosystem. Additionally, synthetic surfactants often have toxicity and biocompatibility issues, and cause harm to ecosystems further limiting their application [11].

Based on findings, the genus *Bacillus* produces lipopeptide-type biosurfactants [12, 13]. Surfactin is a member of the lipopeptide group (among low molecular weight biosurfactants), which has an effective surface tension (ST) reducing effect [14, 15]. *Geobacillus* was reclassified from the genus *Bacillus* in 2001 [16]. *Geobacillus* species are aerobic or facultative anaerobic bacteria that prefer neutral or moderate alkaline pH for cell growth, in a wide temperature range from 35 °C to 76 °C [17]. *Geobacillus* species are having emerging potential applications in microbial enhanced oil recovery [18]. According to some recent reports the biosurfactants synthesized by *Geobacillus* species, are high molecular weight biosurfactants. Their main feature is rather good emulsification than surface tension

Cite this article as: Czinkóczky, R., Németh, Á. "Modeling the Biosurfactant Fermentation by *Geobacillus stearothermophilus* DSM2313", Periodica Polytechnica Chemical Engineering, 67(1), pp. 104–115, 2023. https://doi.org/10.3311/PPch.20797

reduction [14, 15, 18]. These high molecular weight biosurfactants are often considered bioemulsifiers, which do not have good surface activity, but their emulsifying properties are prominent. Bioemulsifiers are generally produced by bacteria in oil reservoirs with high temperatures [18].

As previously discussed, biosurfactants have several advantages and application fields that make them promising alternatives to chemically synthesized surfactants. However, they face some barriers related to low yields, high production costs associated with expensive raw materials, and optimization difficulties. These are the bottlenecks of the large-scale economical production hindering biosurfactants to receive a commercially competitive position [14, 19]. Cheaper substrates have several drawbacks in large-scale production, e.g., required special purification, the raw material composition may vary, and a large quantity of raw substrates is necessary. On the other hand, cheaper substrates are available in huge quantities, the commercial production cost can be reduced and additionally all components could be ecologically friendly and safe [20, 21].

The aim of this paper is to present a rational media optimization approach to enhance the productivity of the biosurfactant production for *Geobacillus stearothermophilus* DSM2313 via response surface methodology. Two central composite designs (CCDs) were carried out until the optimum finding with the highest efficiency. Based on the experimental results an artificial neural network (ANN) was built, tested and validated to predict the biosurfactant fermentation. In the developed ANN two outcome parameters were predicted simultaneously, namely the optical density (for biomass estimation) and the emulsification index (for assuming product formation). These findings contribute to the prediction of an efficient biosurfactant fermentation harvesting time.

2 Materials and methods

2.1 Bacteria and cultivation

Geobacillus stearothermophilus DSM2313 was purchased from the Leibniz Institute DSMZ-German Collection of Microorganisms and Cell Cultures GmbH.

In our experiments, the strain was maintained at 4 °C on Luria-Bertani agar (10.0 g/L tryptone, 5.0 g/L yeast extract, 10 g/L NaCl, 15.0 g/L agar).

2.2 Biosurfactant fermentation

A minimal medium was applied for the biosurfactant fermentation, since its components do not affect the surface tension of the broth, hence the product formation can be monitored by stalagmometric ST measurements. Unless otherwise indicated, all chemicals were purchased from Reanal Laboratory Chemicals Ltd., Hungary. 1 L of minimal media (pH=~6) consisted of 34.0 g glucose (Hungrana Ltd., Szabadegyháza, Hungary), 6.0 g KH_2PO_4, 2.7 g Na_2HPO_4, 1.0 g NH_4NO_3, 0.1 g $MgSO_4 \cdot 7H_2O$, $1.2 \cdot 10^{-3}$ g $CaCl_2$, $1.65 \cdot 10^{-3}$ g $FeSO_4 \cdot 7H_2O$, $1.5 \cdot 10^{-3}$ g $MnSO_4 \cdot 4H_2O$ and $2.2 \cdot 10^{-3}$ g Na-EDTA [22]. The biosurfactant fermentations were conducted in 250 mL shaking flasks. The inoculum, of which media had the same composition as described above, was incubated for 2 days at 150 rpm and 37 °C in a rotary shaker (New Brunswick Excella E24) resulting in an inoculation ratio of 10%. In terms of the applied temperature, but considering a future large-scale application, a lower temperature seemed to be more feasible therefore only 37 °C was applied. During the biosurfactant fermentation, the starting total volume (including the inoculum as well) was 150 mL, and the fermentation parameters were the same, as in case of inoculum.

2.3 Analysis of biomass

The biomass concentration was followed with the optical density (OD) of the fermentation broth measured at a wavelength of 600 nm with a Camspec M501 spectrophotometer against the sample's supernatant after centrifugation at 12,000 rpm 5 min using Heraeus Biofuge Pico Z Eppendorf centrifuge (24·1.5 mL).

2.4 Analysis of glucose

Isocratic high-performance liquid chromatography (HPLC) system (Breeze, Waters) was applied using a Bio-Rad Aminex HPX-87H column at 65 °C with an eluent of 5 mM H_2SO_4 (CARLO ERBA Reagents, Milan, Italy) in ultrapure water (Simplicity, Millipore) and refractive index (RI) detector at 40 °C, an injection volume of 10 µL and mobile phase flow rate of 0.5 mL/min. Glucose calibration ($R^2=1.0$) was prepared before HPLC measurements with two-fold dilution series starting from 10 to 0.3125 g/L, which resulted in the equation (Eq. (1)):

$$\text{Glucose}\left[\frac{\text{g}}{\text{L}}\right] = 4 \cdot 10^{-6} \cdot \text{Peak Area}\left[\text{MV} \cdot \text{s}\right]. \quad (1)$$

2.5 Isolation of the biosurfactant

The purification method of biosurfactants was adapted from Joshi et al. [23]. At the end of the fermentation the cells were removed by centrifugation using Janetzki MLW K23 D (20 mins, 4,000 rpm 4 °C). The pH of the cell-free supernatant was set below 2 with 6 N HCl and was kept in

fridge at 4 °C overnight. The next day this solution which contained the acid precipitate was centrifuged (20 mins, 4,000 rpm, Janetzki MLW K23 D) to separate the acidified product from the supernatant. The supernatant was discarded, the acid precipitate was resuspended, and its pH was set back to 7 by 6 N NaOH. Finally, this neutralized suspension (containing the biosurfactant) was lyophilized, which took approximately 1 day. After the freeze-drying the off-white powder was measured gravimetrically and considered as the isolated crude biosurfactants.

2.6 Surface tension measurements

In order to follow the product formation, stalagmometric surface tension measurements were applied [24]. The surface tension of the samples was measured by a glass stalagmometer (Wilmad Labglass LG5050-100). The formed biosurfactants decreased the surface tension of the broth in comparison to water's surface tension. Three parallel measurements were performed on each sample.

2.7 Emulsifying activity measurements

Emulsification activity was determined by the addition of 2 mL of sunflower oil to the same volume of cell-free sample solutions in a test tube, which was mixed vigorously with a vortex for 2 min [25]. The tubes were incubated at 25 °C, and the emulsification index (EI) and emulsification stability (E24) were determined after t = 1 hour and t = 24 hours, respectively (Eq. (2)):

$$\mathrm{EI}_t = \left(H_e / H_t\right) \cdot 100, \tag{2}$$

where H_e and H_t are the height of emulsion and the total height of the liquid in the tube, respectively.

2.8 Statistical optimization

First, a randomized central composite design (CCD1) was built with the help of Statistica 13.5 software (StatSoft, Inc., Tulsa, USA). A statistical design with 3 factors on two levels (8 corner points) plus two star points per axis (2·3 = 6) and a centrum point with duplicates were generated as overall 16 runs. The overall design was carried out in triplicates resulting in an overall experiment of 48 runs. These were randomized and prepared in 12 flasks in 4 periods.

Since the estimated optimum was not in the investigated range, a second CCD was generated with shifted and wider factor ranges based on CCD1.

The second randomized central composite design (CCD2) was also built with the help of Statistica 13.5 software. For the second design, 3 factors on two levels (8 corner points) plus two star points per axis (2·3 = 6) and a centrum point with duplicates were generated as overall 16 runs again. In CCD2 the factors were investigated at the following low and high levels: glucose 50–80 g/L, NH_4NO_3 2–4 g/L and initial pH of 7–11. The overall design was carried out in duplicates resulting in the overall experiment of 32 runs. These were randomized and divided into 3 parts as 12+12+8 flasks.

In the media composition, the glucose and NH_4NO_3 concentrations as well as the initial pH values were altered. In order to fine-tune the optimum setup (observed from the response surface methodology), 4 additional combinations of the investigated factors were tested in 3 replicates for the bacteria (12 shaking flasks, Table 1).

2.9 Fermentation monitoring

Samples were taken daily to determine the OD and ST, EI and E24 values. Glucose concentrations were measured at starting and final points of the fermentation for the yield calculation. When the OD showed a decrement in the cell growth, it indicated that the cells started spore-forming, and the fermentations were stopped. The duration of the fermentations alternated between 3 and 7 days.

2.10 Kinetic modeling

Berkely Madonna 10.1.3 [26] was applied for kinetic modeling. Curve fitting of Monod model's differential equations was used for the determination of kinetic parameters. Cell growth, glucose consumption and product formation are described in Eqs. (3) to (5), respectively. Monod equation for the substrate dependence of the specific growth rate is described in Eq. (6). In Eqs. (3) to (6) x is related to the optical density at 600 nm [-], μ to the specific growth rate [1/h], $\mu_{\max}$ to the maximal specific growth rate [1/h], K_s to the half saturation constant [g/L], Y to the biomass yield [-], S to the substrate concentration [g/L], k_1 [1/h] and k_2 [-] to the growth independent and growth associated product formation kinetic parameters. The product formation (Eq. (5)) is described by the Luedeking-Piret product formation kinetics.

$$dx / dt = \mu \cdot x \tag{3}$$

$$dS / dt = \left(-1 / Y\right) \cdot \mu \cdot x \tag{4}$$

Table 1 Fine tuning the optimum set up for *G. stearothermophilus* DSM2313

pH [-]	NH_4NO_3 [g/L]	Glucose [g/L]
9	3	70
11	3	70
9	2	50
7	2	50

$$dP / dt = k_1 \cdot x + k_2 \cdot \mu \cdot x \quad (5)$$

$$\mu = \left(\mu_{\max} \cdot S\right) / \left(S + K_S\right) \quad (6)$$

The optimized fermentation datasets were used for the kinetic investigation to determine the kinetic constants from Eqs. (3) to (6), e.g., Y [-], μ_{max} [1/h], K_s [g/L], k_1 [1/h] and k_2 [-]. During the kinetic analysis, the initial values for x [g/L], S [g/L] and P [g/L] were set according to the measurement of the initial samples in the experiments.

2.11 Artificial neural network modeling

Neural networks have universal approximation properties, which means that they can approximate any function in any dimension and up to a desired degree of accuracy. For the ANN modeling, we used Neural Designer 4.2.0 software [27].

The optimization algorithm (Quasi-Newton method) determines how the adjustment of the parameters in the neural network takes place. The optimization algorithm stops when a specified condition is satisfied. The next step is model selection, which minimizes the error on the selected instances of the data set (the selection error). After setting these parameters the training can be started.

Based on the results of CCD 1 and 2 an artificial neural network was created to predict the optimal or the ending time of the fermentation at a certain level of the factors which were investigated in the response surface methodology. The ANN was built for *G. stearothermophilus* DSM2313 with two outcome parameters, namely OD and EI. Emulsification index values provide quickly available information about the emulsifying capability of the sample, therefore we chose that as an outcome parameter instead of E24 values. While E24 values are generally applied, we omitted that from the prediction due to the small changes in the emulsion height with time.

The data set for the biosurfactant production with *Geobacillus stearothermophilus* DSM2313 consisted of 396 instances. For training 238 (60.1%), for testing 79 (19.9%) and for selection 79 (19.9%) instances were used.

We chose the minimum-maximum method for the scaling and unscaling. The perceptron layer comprised 4 layers (3 hidden and 1 output). The hidden layers had hyperbolic tangent activation function, and the output layer had linear activation function. In the training strategy, we set the mean square error for the error method. We applied regularization with a strong weight. We applied the Quasi-Newton method as the optimization algorithm, where the training accuracy was medium (default set). 1,000 were the maximum number of iterations. We set the order selection in incremental order, and we selected the inputs in a growing way. With these settings, we managed to reach as high correlation coefficient for the two outcome parameters as we can.

For the validation of the ANN, four additional different settings were tested (Table 2) in three replicates.

3 Results and discussion

3.1 Media optimization

Throughout the optimization shaking flask experiments, the withdrawn samples were analyzed for OD, ST, emulsification activity and glucose consumption. Before the statistical analysis, the data distribution was checked. The residuals plots indicated that the differences between the measured and fitted values are exhibiting normal distribution and constant variance and are independent of each other (not shown here).

First optimizing design (CCD1) could not conclude to an optimum, therefore only its maximal product formation is introduced here as follows: 1.36 g/L of crude product could be extracted from the best setup of pH = 7, NH_4NO_3 = 2.38 g/L, glucose = 34 g/L. During its fermentation, the maximal surface tension reduction was 8.47 mN/m, meanwhile maximal EI = 58.3% and E24 = 54.7% could be observed, respectively. These results suggested, that the produced surface active agent is rather bioemulsifier, than biosurfactant, which is in good agreement with other *Geobacillus* strains' already described polymer type biosurfactants [14]. Since the highest biomass and product amount was observed in CCD1 at the highest values of the factors, we extended the variables' range in these directions for CCD2.

Fig. 1(A–I) represents the surface plots of CCD2 comprising all parallel runs' results. Each datapoints represents the lowest surface tension value (Fig. 1(A–C). The optimal factor's values are pH = 9, NH_4NO_3 = 4–4.5 g/L and the highest setting (around 90 g/L) is the best for glucose concentration.

On Fig. 1(D–F) each datapoints represents the highest emulsification index (EI) values as the outcome function

Table 2 New validation settings for *Geobacillus stearothermophilus* DSM2313

Initial pH [-]	NH_4NO_3 [g/L]	Glucose [g/L]
8	4	40
8	1.5	10
10	2	40
10	4	50

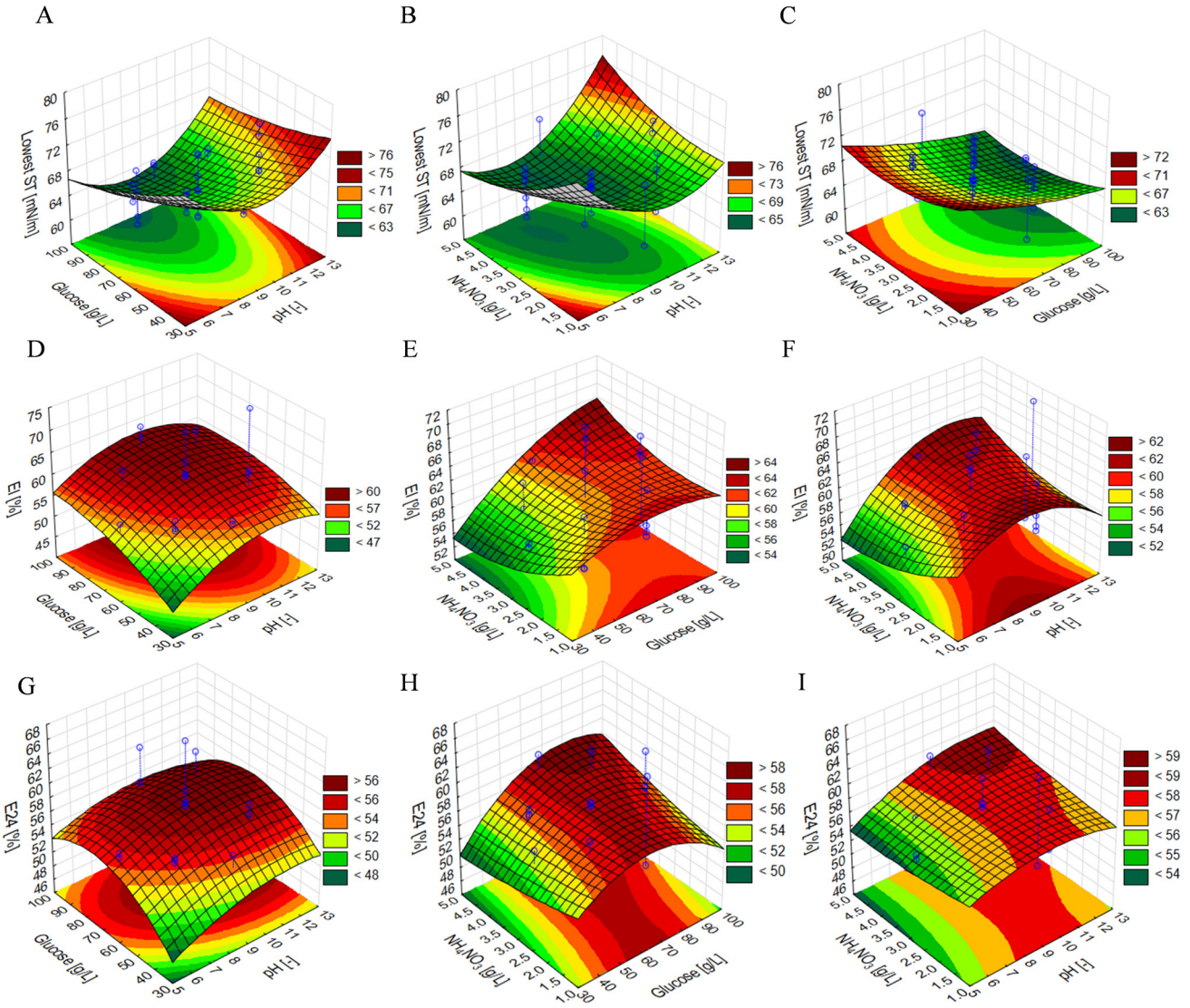

Fig. 1 Surface plots of 2nd central composite design: A-C: Lowest surface tension, D-F: emulsification index, G-I: emulsification stability as outcome parameter (ST: surface tension [mN/m], EI: emulsification index [%], E24: emulsification stability [%])

of the investigated parameters. The optimum can be found at the same setup as for surface tension decrement.

On Fig. 1(G–I) each datapoints represents the highest emulsification stability (E24) values at different levels of the investigated factors. The optimum can be found again at the same setup as for surface tension decrement and emulsification index.

To summarize the result of CCD2 one can conclude, that since the highest EI value (70.5%) decreased slightly after 24 h (E24 = 68.3%) the produced bioemulsifier can form stable emulsions. These highest EI and E24 values were observed at initial pH of 12.5, initial glucose concentration of 65 g/L and initial ammonium-nitrate concentration of 3 g/L.

Despite the result of CCD1 and CCD2 the suggested optimum setups have some application issues, since either lag phase was very long, or residual glucose remarkable at the end of the fermentations. Therefore, fine-tuning of the optimum setups were carried out via designing new runs (Table 1) considering both the CCD's results (with special focus on E24 as shown on Fig.1. (G–I)) and lowest residual glucose concentration as well as shortest lag-phase (Table 3) together with the easiest broth treatment (i.e., centrifugation).

The time-course of the three parallel runs of the best setup among the four re-designed experiments are presented in Fig. 2.

This fermentation took 4 days, but the glucose ran out of the media after around 70 hours. The cell growth initiated on the 1st day and stopped after 3 days. The ST slowly but decreased during the fermentation, it went down from 73 to 60–64 mN/m. The emulsification index increased

Table 3 Experimental settings and results for CCD2

Standard run	Glucose [g/L]	NH_4NO_3 [g/L]	Initial pH	Lowest ST [mN/m]	EI [%]	E24 [%]	Lag phase length [h]	Residual glucose [g/L]
1	50	2	7	70.5 ± 0.5	55.35 ± 0.92	53.8 ± 1.84	0	8.21 ± 0.82
2	50	4	7	67.9 ± 0.7	56.7 ± 1.70	55 ± 0.57	0	0
3	80	2	7	65.2 ± 0.4	59.1 ± 4.38	53.95 ± 1.91	24	0
4	80	4	7	60.9 ± 0.9	57.65 ± 0.64	55.65 ± 0.07	24	0
5	50	2	11	71.0 ± 2.8	58.45 ± 5.44	55.05 ± 4.03	24	0
6	50	4	11	68.1 ± 1.2	57.6 ± 5.80	56.1 ± 0.57	24	0
7	80	2	11	64.5 ± 3.2	56.15 ± 1.20	53.2 ± 0.99	23	0.64 ± 0.01
8	80	4	11	65.9 ± 2.6	62.65 ± 2.76	57.5 ± 4.38	23	0.65 ± 0.01
9	65	3	9	63.7 ± 3.2	59.65 ± 0.35	57.85 ± 0.35	0	0
10	65	3	5.47	69.7 ± 1.9	55 ± 1.41	55.05 ± 0.49	95	1.25
11	65	3	12.53	70.7 ± 0.8	61.6 ± 12.59	59.4 ± 12.59	47	0.40 ± 0.56
12	38.54	3	9	67.0 ± 0.4	56.8 ± 0.42	53.25 ± 2.76	0	0
13	91.46	3	9	65.6 ± 0.2	64.9 ± 1.70	59.2 ± 3.54	0	0
14	65	1.24	9	66.5 ± 6.9	66.2 ± 6.65	60.75 ± 8.41	27	6.37 ± 3.62
15	65	4.76	9	55.8 ± 12.2	60.9 ± 0.28	57.3 ± 3.68	0	0
16	65	3	9	66.9 ± 1.7	61.55 ± 3.75	57 ± 1.70	0	0.11 ± 0.15

* ST: surface tension, EI: emulsification index, E24: emulsification stability

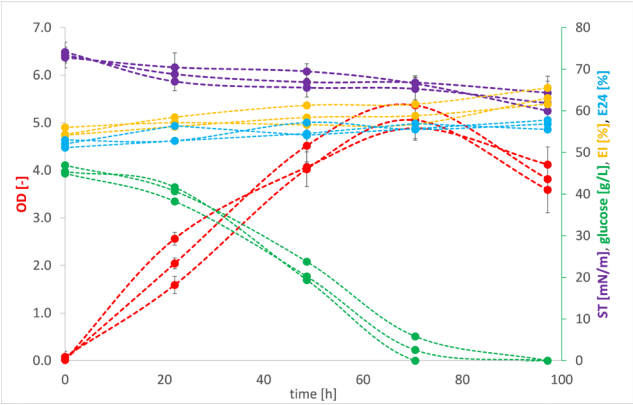

Fig. 2 Optimum setting for *G. stearothermophilus* DSM2313 (50 g/L glucose, 2 g/L NH4NO3, pH=7), where OD: optical density, ST: surface tension, EI: emulsification index and E24: emulsification stability)

from 54% to 65%, confirming that the biosurfactant is an appropriate candidate as an emulsifier. The E24 values increased parallel with the EI values, which indicates the formation of a stable emulsifier in the broth.

Compared to the handful reports on biosurfactant production with *G. stearothermophilus*, the UCP 986 strain was able to synthesize a 2.3 g/L surface-active product (isolated with an acetone precipitation method) on corn steep liquor and palm oil, which was able to reduce the ST from 72 to 31 mN/m. The product's average emulsification index alternated between 30–35 % (against corn oil, diesel and vegetable fat post frying oil) and 85 % (against engine burning oil) [1]. Compared to our results the DSM2313 strain has a better emulsification activity on vegetable oil. Another *G. stearothermophilus* SR-1 strain was cultivated on a rich medium containing mainly glucose, yeast extract and peptone for about 15 days. Its product was able to reduce the ST, with about a ΔST_{max} of 33 mN/m. The cell-free supernatant of this strain had an emulsification index of EI=60% against crude oil, which was evaluated by the authors as a good bioemulsifier [18]. Furthermore, *G. stearothermophilus* strain A-2 has also shown potential bioemulsifier production and hydrocarbon degradation. It was able to emulsify oil on a basal salts medium supplemented with yeast extract [28].

To conclude our investigated *G. stearothermophilus* DSM2313 strain proved to be an effective emulsifier producer compared to other reports. During its fermentation, the emulsification index rose from 50% up to 65% against vegetable oil.

3.2 Kinetic investigation

Based on the raw data of Fig. 2, a kinetic analysis was performed (Fig. 3) applying Berkeley Madonna software. Table 4 represents the initial value of model parameters, which were changed during the curve fitting analysis. During the curve fitting, the constant parameters were adjusted by the software to reach the smallest root mean square (RMS) value. RMS indicates the difference between the fitted functions and the measured data points. This value started at 5.9 and decreased to 3.8 at the end of

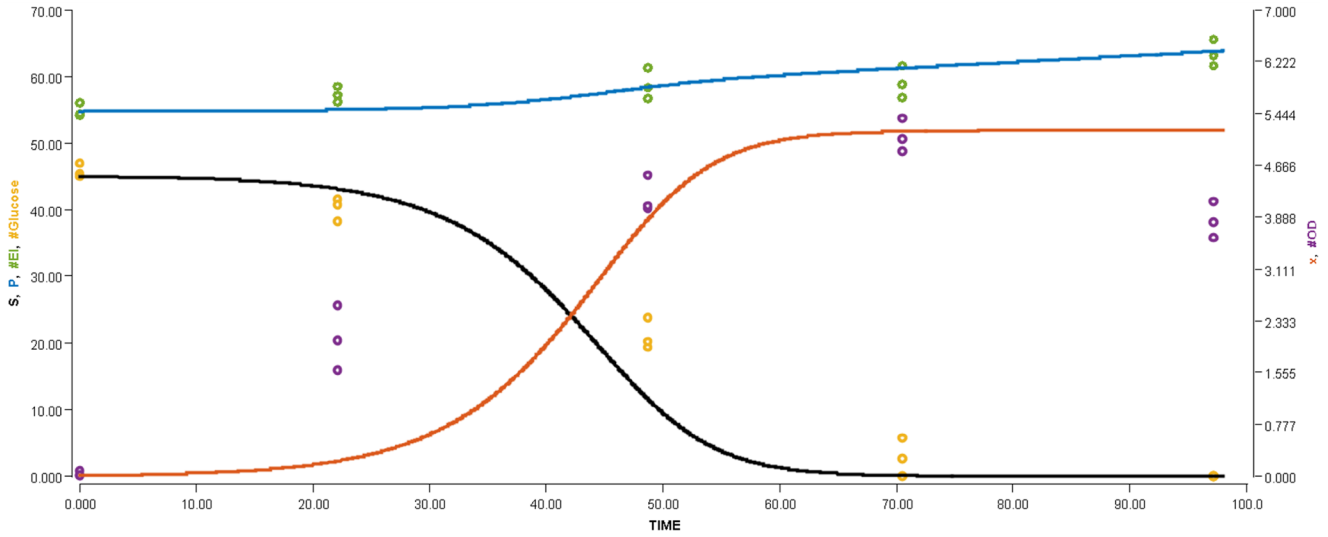

Fig. 3 Kinetic fermentation profile of G. stearothermophilus DSM2313 (Measured values: green circles-EI, yellow circles-glucose concentration, purple circles-OD. Fitted functions: blue line-EI, black line-glucose, red line-OD). *S* (substrate) [g/L] is the fitted function for glucose [g/L], *P* (product) [g/L] is the fitted function for EI (emulsification index) [%] and *x* (biomass) [g/L] is fitted function for OD (optical density) [-].

Table 4 Kinetic parameters after curve fitting

Parameter	After curve fitting
μ_{max} [1/h]	0.31
K_S [g/L]	59
Y [-]	0.115
k_1 [1/h]	0.018
k_2 [-]	0.731

the curve fitting, which indicates, that the model describes the fermentation with small variation. Biosurfactant production proved to be evaluated as a growth associated product formation according to the kinetic parameters, since the growth associated (k_2) is significantly higher than zero, meanwhile and the non-growth-associated (k_1) parameter is very close to zero.

Some reported initiatives modeled the biosurfactant production by *Bacillus* species. In a study with *Bacillus circulans* two media were compared, where the biomass yield (Y) was at about 0.2 and the product formation was parallel with the cell growth as well [29]. In terms of specific growth rate 0.2–0.3 1/h is generally observed on inorganic media for many different *Bacilli* in different product formations. However, on inorganic media for *B. licheniformis* biosurfactant fermentation 0.026 1/h growth rate was observed [30]. According to a study with *B. subtilis*, the surfactin production is described as partial growth associated [31]. Monod and Luedeking-Piret models are frequently applied for the determination of cell growth and biosurfactant product formation, however in some cases some modifications required (combination with logistic model) [30, 32–34].

3.3 Artificial neural network

The quasi-Newton method training strategy is applied to the neural network to obtain the best possible loss. Fig. 4(A) shows the training and selection errors in each iteration. The blue line represents the training error and the orange line represents the selection error, where both errors were similar. The initial training error value of 7.903 decreased to 0.076 after 551 epochs. Meanwhile, the initial value of the selection error decreased from 7.512 to 0.101. Incremental order (Fig. 4(B)) is used here as an order selection algorithm in the model selection, the blue line represents the training error and the orange line symbolizes the selection error. The optimum order was number 3 based on the small difference between the training and selection errors; where the optimum training error was 0.080, and the optimum selection error was 0.105, and the iteration number was 9.

A graphical representation of the resulted deep architecture is in Fig. 4(E). It contains a scaling layer, a neural network and an unscaling layer. The yellow circles represent scaling neurons, the blue circles the perceptron neurons and the red circles the unscaling neurons. The number of inputs is 4, and the number of outputs is 2. The complexity, represented by the number of hidden neurons, is 6:6:3.

After training of ANN, the linear regression analysis was performed. On the linear regression chart of optical density (Fig. 4(C)), the predicted values are plotted versus

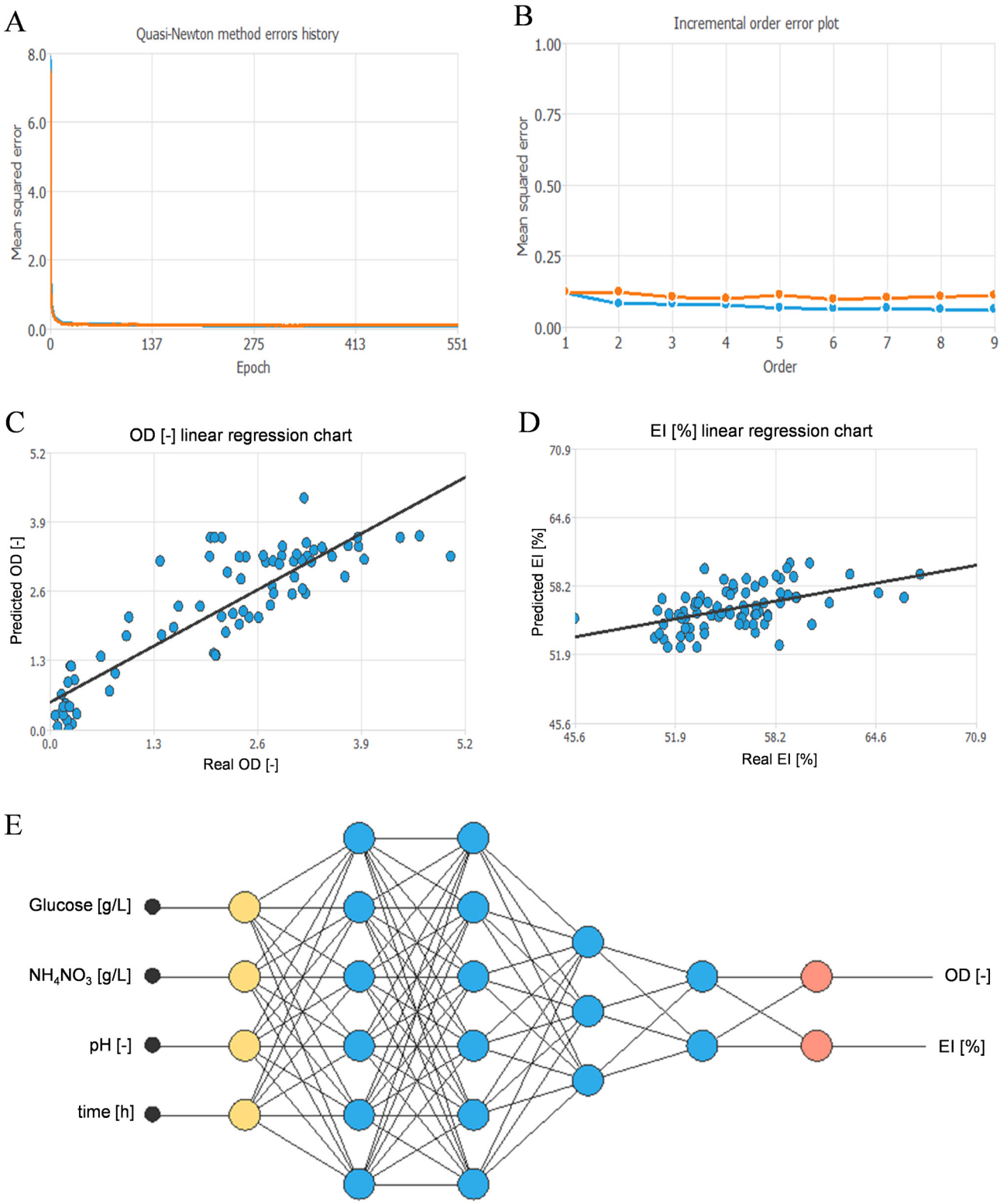

Fig. 4 Artificial neural network with *Geobacillus stearothermophilus* DSM2313; A: Quasi-Newton method errors history; B: Incremental error plot; C: Linear regression chart for optical density (OD) (intercept:0.513; slope:0.813; correlation:0.877); D: Linear regression chart for emulsification index (EI) (intercept:41.6; slope:0.261; correlation:0.5); E: Artificial neural network structure for OD and EI

the measured ones. In Fig. 4(D) the linear regression chart of EI is presented. In Fig. 4(C) and (D), the black lines were indicated as the best linear fit according to the build ANN.

The measured and the predicted parameters are represented in Fig. 5. The correlation value for biomass growth was quite acceptable (0.877). Despite the low correlation

value (0.5) for EI in the case of *G. stearothermophilus* DSM2313, the ANN predicts the EI changes quite well during the fermentation.

Analyzing the data distribution and the box plots in Fig. 6(A–D) it can be seen that the optical density values have a wide data distribution in the whole range (i.e., between minimum and maximum value of OD). Therefore, the correlation values can be higher than in the case of the emulsification index values, where only a narrow range is covered by most of the EI data, which suggests, that EI is not a sensitive parameter against the examined factors.

MATLAB is a frequently applied software for building artificial neural networks [35] and machine-learning models [36]. Among the research papers with artificial neural networks both for biosurfactant production and any other fermentation product, usually, only one outcome parameter is investigated [37], and if one would like to predict any additional fermentation result parameter, another ANN is built instead of applying two or more outcome parameters simultaneously [38], like in the case of biosurfactant production with *Klebsiella* sp. FKOD36 [39].

Here we have presented a software for building an artificial neural network, of which application in the field of biosurfactant production has not been published yet elsewhere. Neural Designer is easy to use tool for modeling and predicting two outcome parameters simultaneously, namely the cell growth together with surface tension or emulsification index alteration during the fermentations. These

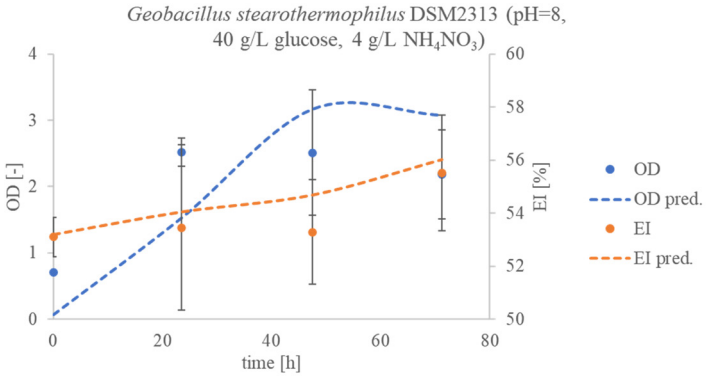

Fig. 5 Fermentation prediction for optical density (OD) and emulsification index (EI)

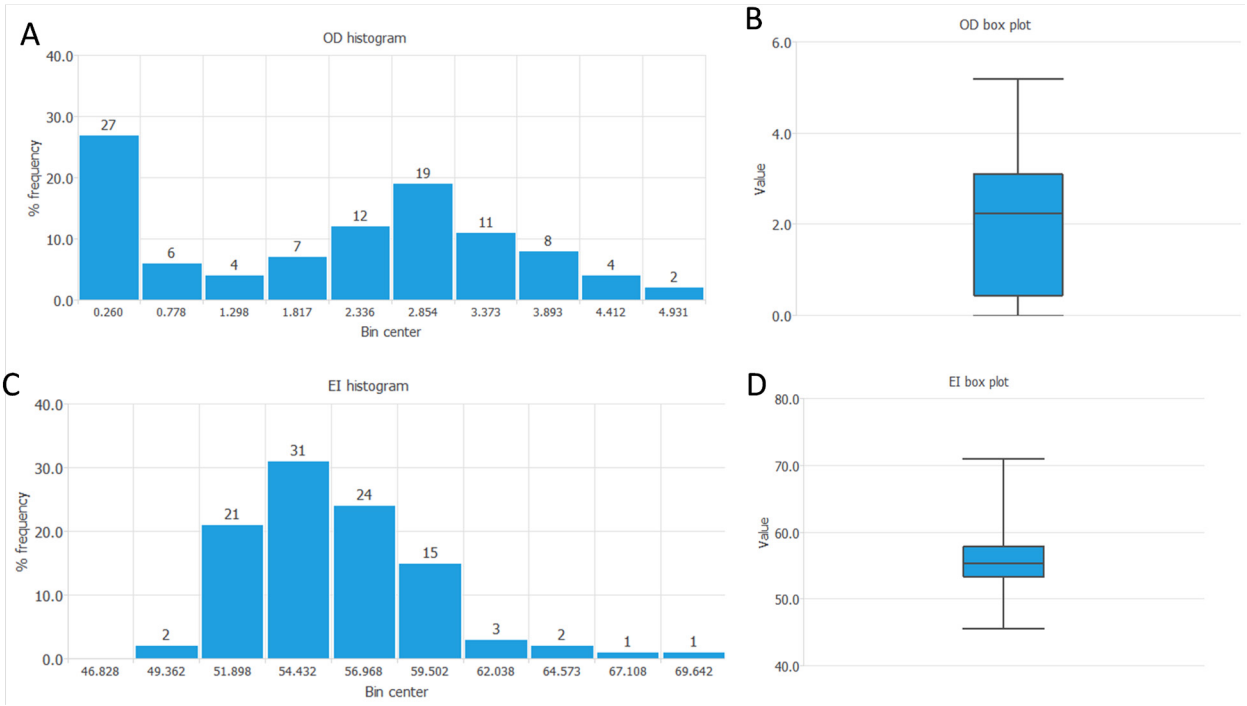

Fig. 6 Data distribution and box plots for optical density (OD) and for emulsification index (EI); A: OD histogram; B: OD box plot; C: EI histogram; D: EI box plot

results contribute to the forward prediction of the product efficiency and the harvesting time of the fermentation broth, which can enhance the fermentations' productivity.

4 Conclusion

The research has shown that *Geobacillus stearothermophilus* DSM2313 is an appropriate producer of an effective tensio-active, which was here first characterized as bioemulsifier. With the help of response surface methodology and artificial neural network we are able to predict simultaneously the product and biomass formation, additionally, the harvesting time of the fermentation. These findings may contribute to the microbial enhanced oil recovery. Further improvement needs to be done before large-scale application to solve the foaming problem in fermenters.

Acknowledgement

This work was supported by the Gedeon Richter's Talentum Foundation, founded by Gedeon Richter Plc., Gedeon Richter PhD fellowship. The research reported in this paper and carried out at BME has been supported by the NRDI Fund (TKP2020 NC, Grant No. BME-NC) based on the charter of bolster issued by the NRDI Office under the auspices of the Ministry for Innovation and Technology.

References

[1] Jara, A. M. A. T., Andrade, R. F. S., Campos-Takaki, G. M. "Physicochemical characterization of tensio-active produced by *Geobacillus stearothermophilus* isolated from petroleum-contaminated soil", Colloids and Surfaces B: Biointerfaces", 101, pp. 315–318, 2013. https://doi.org/10.1016/j.colsurfb.2012.05.021

[2] Thangadurai, D., Sangeetha, J. (eds.) "Industrial Biotechnology: Sustainable Production and Bioresource Utilization", Apple Academic Press, 2017. ISBN 9781315366562 https://doi.org/10.1201/9781315366562

[3] Naughton, P. J., Marchant, R., Naughton, V., Banat, I. M. "Microbial biosurfactants: current trends and applications in agricultural and biomedical industries", Journal of Applied Microbiology, 127(1), pp. 12–28, 2019. https://doi.org/10.1111/jam.14243

[4] Marchant, R., Banat, I. M. "Biosurfactants: a sustainable replacement for chemical surfactants?", Biotechnology Letters, 34(9) pp. 1597–1605, 2012. https://doi.org/10.1007/s10529-012-0956-x

[5] Shekhar, S., Sundaramanickam, A., Balasubramanian, T. "Biosurfactant Producing Microbes and their Potential Applications: A Review", Critical Reviews in Environmental Science and Technology, 45(14), pp. 1522–1554, 2015. https://doi.org/10.1080/10643389.2014.955631

[6] Santos, D. K. F., Rufino, R. D., Luna, J. M., Santos, V. A., Sarubbo, L. A. "Biosurfactants: Multifunctional Biomolecules of the 21st Century", International Journal of Molecular Sciences, 17(3), 401, 2016. https://doi.org/10.3390/ijms17030401

[7] Gudiña, E. J., Rangarajan, V., Sen, R., Rodrigues, L. R. "Potential therapeutic applications of biosurfactants", Trends in Pharmacological Sciences, 34(12), pp. 667–675, 2013. https://doi.org/10.1016/j.tips.2013.10.002

[8] Smith, M. L., Gandolfi, S., Coshall, P. M., Rahman, P. K. S. M. "Biosurfactants: A Covid-19 Perspective", Frontiers in Microbiology, 11, 1341, 2020. https://doi.org/10.3389/fmicb.2020.01341

[9] Inamuddin, Ahamed, M. I., Prasad, R. (eds.) "Microbial Biosurfactants: Preparation, Properties and Applications", Springer, 2021. ISBN 978-981-15-6606-6 https://doi.org/10.1007/978-981-15-6607-3

[10] Markande, A. R., Patel, D., Varjani, S. "A review on biosurfactants: properties, applications and current developments", Bioresource Technology, 330, 124963, 2021. https://doi.org/10.1016/j.biortech.2021.124963

[11] Sarubbo, L. A., Silva, M. da G. C., Durval, I. J. B., Bezerra, K. G. O., Ribeiro, B. G., Silva, I. A., Twigg, M. S., Banat, I. M. "Biosurfactants: Production, properties, applications, trends, and general perspectives", Biochemical Engineering Journal, 181, 108377, 2022. https://doi.org/10.1016/j.bej.2022.108377

[12] Jha, S. S., Joshi, S. J., Geetha, S. J. "Lipopeptide production by *Bacillus subtilis* R1 and its possible applications", Brazilian Journal of Microbiology, 47(4), pp. 955–964, 2016. https://doi.org/10.1016/j.bjm.2016.07.006

[13] Dimkić, I., Stanković, S., Nišavić, M., Petković, M., Ristivojević, P., Fira, D., Berić, T. "The Profile and Antimicrobial Activity of *Bacillus* Lipopeptide Extracts of Five Potential Biocontrol Strains", Frontiers in Microbiology, 8, 925, 2017. https://doi.org/10.3389/fmicb.2017.00925

[14] Vieira, I. M. M., Santos, B. L. P., Ruzene, D. S., Silva, D. P. "An overview of current research and developments in biosurfactants", Journal of Industrial and Engineering Chemistry, 100, pp. 1–18, 2021. https://doi.org/10.1016/j.jiec.2021.05.017

[15] Fenibo, E. O., Douglas, S. I., Stanley, H. O. "A Review on Microbial Surfactants: Production, Classifications, Properties and Characterization", Journal of Advances in Microbiology, 18(3), pp. 1–22, 2019. https://doi.org/10.9734/jamb/2019/v18i330170

[16] Nazina, T. N., Tourova, T. P., Poltaraus, A. B., Novikova, E. V., Grigoryan, A. A., Ivanova, A. E., Lysenko, A. M., Petrunyaka, V. V., Osipov, G. A., Belyaev, S. S., Ivanov, M. V. "Taxonomic study of aerobic thermophilic bacilli: descriptions of Geobacillus subterraneus gen. nov., sp. nov. and Geobacillus uzenensis sp. nov. from petroleum reservoirs and transfer of Bacillus stearothermophilus, Bacillus thermocatenulatus, Bacillus thermoleovorans, Bacillus kaustophilus, Bacillus thermodenitrificans to Geobacillus as the new combinations G. stearothermophilus, G. th.", International Journal of Systematic and Evolutionary Microbiology, 51(2), pp. 433–446, 2001.
https://doi.org/10.1099/00207713-51-2-433

[17] Wada, K., Suzuki, H. "Chapter 15 - Biotechnological platforms of the moderate thermophiles, *Geobacillus* species: notable properties and genetic tools", In: Salwan, R., Sharma, V. (eds.) Physiological and Biotechnological Aspects of Extremophiles, Academic Press, 2020, pp. 195–218. ISBN 978-0-12-818322-9
https://doi.org/10.1016/B978-0-12-818322-9.00015-0

[18] Hongyan, H., Weiyao, Z., Zhiyong, S., Ming, Y. "Mechanisms of oil displacement by *Geobacillus stearothermophilus* producing bio-emulsifier for MEOR", Petroleum Science and Technology, 35(17), pp. 1791–1798.
https://doi.org/10.1080/10916466.2017.1320675

[19] Singh, P., Patil, Y., Rale, V. "Biosurfactant production: emerging trends and promising strategies", Journal of Applied Microbiology, 126(1), pp. 2–13, 2019.
https://doi.org/10.1111/jam.14057

[20] Banat, I. M., Satpute, S. K., Cameotra, S. S., Patil, R., Nyayanit, N. V. "Cost effective technologies and renewable substrates for biosurfactants' production", Frontiers in Microbiology, 5, 697, 2014.
https://doi.org/10.3389/fmicb.2014.00697

[21] Jimoh, A. A., Lin, J. "Biosurfactant: A new frontier for greener technology and environmental sustainability", Ecotoxicology and Environmental Safety, 184, 109607, 2019.
https://doi.org/10.1016/j.ecoenv.2019.109607

[22] Joshi, S. J., Geetha, S. J., Yadav, S., Desai, A. J. "Optimization of Bench-Scale Production of Biosurfactant by *Bacillus Licheniformis* R2", APCBEE Procedia, 5, pp. 232–236, 2013.
https://doi.org/10.1016/j.apcbee.2013.05.040

[23] Joshi, S. J., Geetha, S. J., Desai, A. J. "Characterization and Application of Biosurfactant Produced by *Bacillus licheniformis* R2", Applied Biochemistry and Biotechnology, 177(2), pp. 346–361, 2015.
https://doi.org/10.1007/s12010-015-1746-4

[24] Czinkóczky, R., Németh, Á. "The Effect of pH on Biosurfactant Production by Bacillus Subtilis DSM10", Hungarian Journal of Industry and Chemistry, 48(2), pp. 37–43, 2020.
https://doi.org/10.33927/hjic-2020-25

[25] Vaz, D. A., Gudiña, E. J., Alameda, E. J., Teixeira, J. A., Rodrigues, L. R. "Performance of a biosurfactant produced by a *Bacillus subtilis* strain isolated from crude oil samples as compared to commercial chemical surfactants", Colloids and Surfaces B: Biointerfaces, 89, pp. 167–174, 2012.
https://doi.org/10.1016/j.colsurfb.2011.09.009

[26] Berkeley Madonna, Inc. "Berkeley Madonna (10.1.3)", [computer program] Available at: https://berkeley-madonna.myshopify.com/ [Accessed: 16 November 2020]

[27] Artificial Intelligence Techniques, Ltd. "Neural Designer (4.2.0)", [computer program] Available at: https://www.neuraldesigner.com/ Accessed [28 March 2020]

[28] Zhou, J.-F., Gao, P.-K., Dai, X.-H., Cui, X.-Y., Tian, H.-M., Xie, J.-J., Li, G.-Q., Ma, T. "Heavy hydrocarbon degradation of crude oil by a novel thermophilic *Geobacillus stearothermophilus* strain A-2", International Biodeterioration & Biodegradation, 126, pp. 224–230, 2018.
https://doi.org/10.1016/j.ibiod.2016.09.031

[29] Sivapathasekaran, C., Mukherjee, S., Sen, R. "Biosurfactant production and growth kinetics of bacteria in a designer marine medium: Improved physiochemical properties", Biotechnology Journal, 5(10), pp. 1060–1068, 2010.
https://doi.org/10.1002/biot.201000175

[30] Amodu, O. S., Ojumu, T. V., Ntwampe, S. K. O. "Kinetic modelling of cell growth, substrate utilization, and biosurfactant production from solid agrowaste (*Beta vulgaris*) by *Bacillus licheniformis* STK 01", The Canadian Journal of Chemical Engineering, 94(12), pp. 2268–2275, 2016.
https://doi.org/10.1002/cjce.22631

[31] Rocha, P. M., dos Santos Mendes, A. C., de Oliveira Júnior, S. D., de Araújo Padilha, C. E., de Sá Leitão, A. L. O., da Costa Nogueira, C., de Macedo, G. R., dos Santos, E. S. "Kinetic study and characterization of surfactin production by *Bacillus subtilis* UFPEDA 438 using sugarcane molasses as carbon source", Preparative Biochemistry & Biotechnology, 51(3), pp. 300–308, 2021.
https://doi.org/10.1080/10826068.2020.1815055

[32] Rodrigues, L., Moldes, A., Teixeira, J., Oliveira, R. "Kinetic study of fermentative biosurfactant production by *Lactobacillus* strains", Biochemical Engineering Journal, 28(2), pp. 109–116, 2006.
https://doi.org/10.1016/j.bej.2005.06.001

[33] Das, S., Sen, R. "Kinetic modeling of sporulation and product formation in stationary phase by *Bacillus coagulans* RK-02 vis-à-vis other *Bacilli*", Bioresource Technology, 102(20), pp. 9659–9667, 2011.
https://doi.org/10.1016/j.biortech.2011.07.067

[34] Petelkov, I., Shopska, V., Denkova-Kostova, R., Ivanova, K., Kostov, G., Lyubenova, V. "Investigation of Fermentation Regimes for the Production of Low-alcohol and Non-alcohol Beers", Periodica Polytechnica Chemical Engineering, 65(2), pp. 229–237, 2021.
https://doi.org/10.3311/PPch.15975

[35] Zhang, A.-H., Zhu, K.-Y., Zhuang, X.-Y., Liao, L.-X., Huang, S.-Y., Yao, C.-Y., Fang, B.-S. "A robust soft sensor to monitor 1,3-propanediol fermentation process by *Clostridium butyricum* based on artificial neural network", Biotechnology and Bioengineering, 117(11), pp. 3345–3355, 2020.
https://doi.org/10.1002/bit.27507

[36] Jovic, S., Guresic, D., Babincev, L., Draskovic, N., Dekic, V. "Comparative efficacy of machine-learning models in prediction of reducing uncertainties in biosurfactant production", Bioprocess and Biosystems Engineering, 42(10), pp. 1695–1699, 2019.
https://doi.org/10.1007/s00449-019-02165-y

[37] Sivapathasekaran, C., Sen, R. !Performance evaluation of an ANN-GA aided experimental modeling and optimization procedure for enhanced synthesis of marine biosurfactant in a stirred tank reactor", Journal of Chemical Technology and Biotechnology, 88(5), pp. 794–799, 2013.
https://doi.org/10.1002/jctb.3900

[38] Vidra, A., Németh, Á. "Applicability of Neural Networks for the Fermentation of Propionic Acid by *Propionibacterium acidipropionici*", Periodica Polytechnica Chemical Engineering, 66(1), pp. 10–19, 2022.
https://doi.org/10.3311/PPch.18283

[39] Ahmad, Z., Crowley, D., Marina, N., Jha, S. K. "Estimation of biosurfactant yield produced by *Klebseilla* sp. FKOD36 bacteria using artificial neural network approach", Measurement, 81, pp. 163–173, 2016.
https://doi.org/10.1016/j.measurement.2015.12.019